

EXPERIMENTAL STUDY OF MICROMACHINED CIRCUITS

Rhonda Franklin Drayton and Linda P.B. Katehi
NASA Center for Space Terahertz Technology
University of Michigan
Ann Arbor, MI 48109-2122

1.0 Abstract

Planarization of transmission lines such as microstrip, stripline, and coplanar provide enhanced flexibility in array design, compatibility to active devices and radiating elements, as well as reduced volume and weight. However, many unwanted frequency dependent mechanisms are introduced from these planar lines which cause degradation in the electrical performance of the circuit. As a result, the development of new geometries which reduce the effect of such mechanisms as ohmic loss and electromagnetic interference without affecting the monolithic character will result in extended operating frequencies and improved electrical performance of circuits and arrays. This paper presents the development of micromachined circuits which provide shielding of conventional lines using micromachining techniques. Presented is a description of the fabrication and characterization of these circuits. In addition, the study will show information about the propagation characteristics of the line and scattering parameters for a variety of micromachined circuits with comparison to theoretical and conventional circuit geometries.

2.0 Introduction

The thrust for the development of cost effective, lightweight electrical systems which exhibit improved electrical performance can be attributed to communications, commercial and military applications. One application in the area of communications is for the development of miniature satellites, microsats, which contribute to reduction in weight and improved fuel economy. Commercial applications will benefit from this development of high intelligence highway systems which require parallel processing of vast amounts of information transfer to maintain efficient operation of such systems. On the other hand, military applications will require development of PIN cards used for identifying military personnel. Thus, the impetus for investigating micromachined circuits is due to the strong desire to develop inexpensive circuits that provide improved electrical performance with reduced volume and weight.

Currently, monolithic quasi-planar geometries which exhibit electrical and geometrical resemblance to waveguide shielded transmission lines and circuits are possible to implement due to recent advances in semiconductor processing techniques. Silicon based monolithic waveguides have been successfully developed for use in the sub-millimeter wave frequencies using silicon

micromachining techniques by JPL [1] and University of Michigan[2]. The waveguide is split along the broad wall and each half is formed by etching a channel through an appropriately oriented silicon wafer. Finally, a polyamide bonding technique is used to glue the etched channels to a smooth silicon wafer. In addition their performance has been measured and has been found very satisfactory[1].

Similarly, a shielded transmission line structure, Figure 1, can be developed by replacing the waveguide with a cavity which is etched into Si using KOH and then metallized using evaporation techniques. Then the planar transmission line is created by metal deposition on the Si semiconductor substrate and attached to the original wafer using electrobonding techniques. The results are lines and circuits which evolve from the conventional metallic waveguide and waveguide-shielded components with the advantages mentioned above.

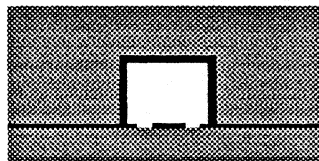


FIGURE 1. Micromachined CPW

As a result, this study will present the development of micromachined circuit, which use an etched cavity as a shield to planar geometries. After describing the fabrication and experimental procedures needed to characterize these novel circuits, scattering parameter measurements will be shown. Finally, results regarding the propagating characteristics of the line and a variety of circuit geometries will be presented and compared to theoretical models as well as conventional geometries.

3.0 Fabrication Procedure

In order to implement the development of a micromachined circuits, technology resulting from recent advances in semiconductor processes is used. These circuits are created by attaching the shielding structure to the planar line structure using electrobonding techniques. Although the shield and lines require the use of standard photolithography, the planar lines use a bilayer process technique for metal definition while the shield uses anisotropic wet etching methods for the development of the cavity structure.

Initially, a Si wafer having a membrane ($SiO_2/Si_3N_4/SiO_2$) dielectric surface is used to develop the cavity structure since depths of varying heights are required. Using photolithography to define the areas to be etched, the first oxide layer is etched using BHF while the nitride layer is etched using plasma etching. After repatterning the wafer to protect the areas to be etched later, the second oxide layer is removed while the remaining membrane layers serve as a mask for any unpatterned sections of wafer. Once the initial depth is obtained for the alignment marks, the remaining cavity areas are then exposed and etched to the required depth. The result is the development of a structure which has sections etched entirely through the wafer, the alignment marks,

and sections etched partially through, the cavities. Once the etch is complete, the shielding portion of the micromachined circuit is metallized using evaporation techniques.

Secondly, transmission lines are designed which consist of calibration standards and various circuit geometries necessary to characterize the electrical performance of the micromachined circuits. The lines, developed on a separate wafer, use photolithography to pattern circuit areas and the bilayer process to develop the appropriate line depth and width with the use of evaporation techniques.

Lastly, the micromachined circuits are developed by aligning the cavity structure to the transmission line structure. Once aligned, they are secured using electrobonding methods.

4.0 Measurement Procedure

Characterization of the circuits require the use of the following experimental arrangement: an HP 8510B Network Analyzer modified to operate up to 40 GHz, an Alessi Probe Station, and Cascade Probe Tips. To reduce the effects of possible substrate modes in the high resistivity silicon substrate, the circuits are isolated from the wafer chuck by 1/8" thick 5880 duroid, $\epsilon_r=2.2$.

To accurately measure the circuit performance of the micromachined circuits, the Thru-Reflect-Line (TRL) calibration technique is used. In order to perform this calibration, standards were fabricated using the above process. A one tier de-embedding technique was used for on-wafer calibration which calibrates the system reference plane along the transmission line. As a result, the calibration takes into account all transitions between the ANA and the reference plane.

The micromachined circuit, Figure 2, requires several transitions along the feed line to excite the micromachined circuit. The first transition is a taper between two 50 ohm sections of cpw-line. This transition is necessary to provide excitation to the desired line via the Cascade 150 μm pitch probes with minimal mismatch to the probes. The input port, having center conductor width of 100 μm and slot width of 60 μm , is transitioned into a line with center conductor width of 180 μm and slot width of 130 μm . The second transition occurs between cpw and micromachined cpw circuit. The micromachined circuit is of coplanar type line which includes a micromachined shielding cavity having height of 200 μm and width of 800 μm . Subsequently, the required input line of all circuits measured will be of this type.



FIGURE 2. Micromachined circuit with various transitions

5.0 Measurements and Discussion

5.1 Philosophy of the Experimental Study

In order to facilitate a complete preliminary study of micromachined circuits, it is necessary to compare the measured results to both theoretical models as well as conventional geometries.

The *theoretical model* used for the micromachined circuits is based on the space domain integral equation (SDIE). With the appropriate Green's function for the lower half space and upper cavity region of the two dimensional circuit, unknown magnetic surface currents used to replace the slots, M_s , can be determined for a given electric source, J_s , using the method of moments. Once M_s is known, Galerkin's method is applied to reduce the above integral equation to a linear system of equations. For a given field distribution, the scattering parameters of the equivalent network is computed using standard techniques. [3,4]

The *coplanar waveguide* circuits, Figure 3b, are design to be identical in geometry to the micromachined planar circuits, Figure 3a. However, the design includes separate calibration standards for the cpw and micromachined circuits.

The resulting measurement will therefore show the response of micromachined circuits as compared to the theoretical model and conventional coplanar waveguide.



FIGURE 3. (a) Micromachined Circuits and (b) Open CPW Circuits

5.2 Measurements

A through line is used to provide information about the propagating characteristics of the micromachined transmission line. Figure 4 below shows the effective dielectric of a line having length of $2088\mu\text{m}$ and dimensions as stated above. The results show good agreement between the measured micromachined circuit and the theoretical model, which is based on Full Wave Analysis[3].

The two circuit designs presented are an open end series stub in Figure 5a, designed to have gap spacing of $30\mu\text{m}$, and open end gap in Figure 5b, designed to resonate at 30 GHz with resonate stub length of $1086\mu\text{m}$

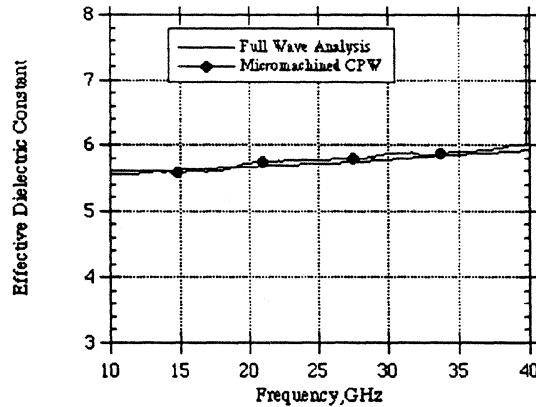


FIGURE 4. Effective Dielectric Constant

and slot width of 30 μm . The scattering parameters for the above circuits have been measured and are compared to the theoretical model for the micromachined cpw circuit. In addition they are compared to conventional cpw circuits of the same type.



FIGURE 5. (a) Open End Series Stub and (b) Open End Gap

For the open end series stub in Figure A1.a, theory and experiment are in excellent agreement both in magnitude and phase as seen in Figures A1.b and A1.c. For the same circuit, comparison with the cpw line is shown in Figures A2.a and A2.b. The line geometry is identical for both circuits, however, the micromachined circuit provides a shielding environment. In Figure A2.c, the total loss of this micromachined circuit varies between 6 dB and 2 dB at the high end below that of conventional cpw lines.

The open end gap in Figure B1.a, shows very close agreement in magnitude and phase with the theoretical results as seen in Figures B1.b and B1.c. As stated initially, it is very important to avoid distortion of the circuit performance when the shield is included. As a result of Figures B2.a and B2.b, comparison between the micromachined circuit and cpw show similarities in the overall circuit performance. The distinction between the lines occur when observing the total loss of the circuits. In Figure B2.c, the total loss, which is again reduced, indicates improvement in the overall performance of the circuit due to the micromachined cavity of the line.

To indicate the potential for this technology, Figure 6 shows a geometrical description of a -milled circuit as compared to the new micromachined circuits. The milled represents one circuit while the micromachined circuit represents 5 different circuits housed on the silicon wafer that is about 1/6 of a 3" wafer.

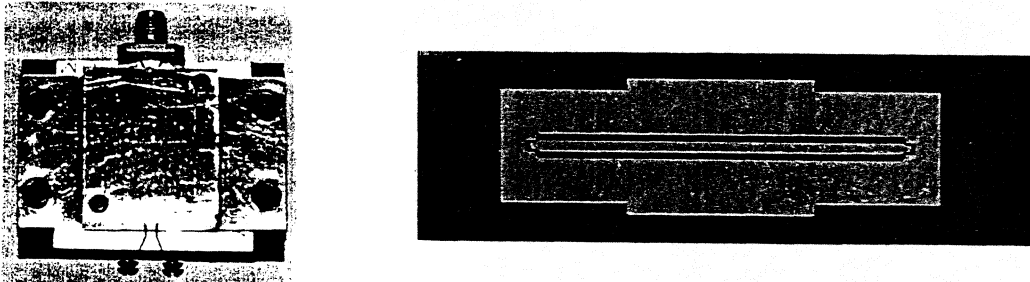


FIGURE 6. Milled Circuit and Micromachined Circuit

In addition to the physical reduction in the size and volume, circuit geometries of similar type indicate promise for applications at terahertz frequencies. However, of the two, the micromachined circuits offer the most flexibility in testing due to state of the art measurement systems available namely the probe station. These circuits and system offer more repeatable measurements along with ease in the fabrication methods used. Figure 7 shows the loss performance of similar geometries between the micromachined and milled circuit. Since the circuits are passive in nature, losses, except ohmic, can be scaled appropriately to the terahertz frequencies to give reasonable indicators of expected circuit performance.

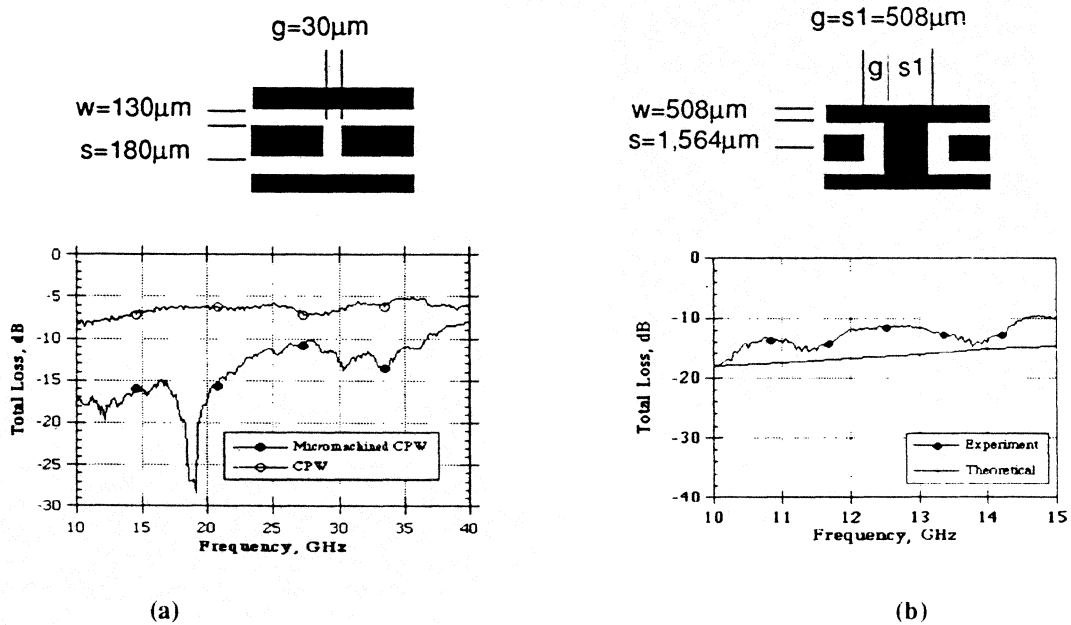


FIGURE 7. Losses of (a) Micromachined circuit vs. (b) Milled circuit

6.0 Summary

Micromachined circuits have been built and tested. The results show that the scattering parameter measurements are in very good agreement with the theoretical model used. The study also shows comparison between the cpw and micromachined cpw. The results indicate consistently that the shielded geometry results in reduction in the total loss of the various circuits measured. When compared to machine milled circuits of similar geometry, the losses are comparable. As a result, micromachined circuits show encouraging preliminary results which warrant further development of these lines for more complicated geometries.

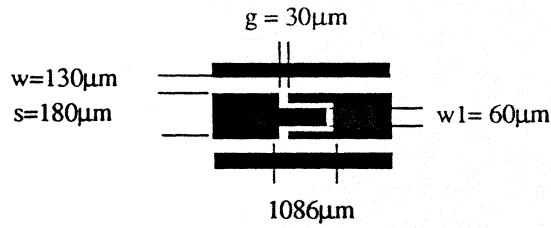
Acknowledgments

This work was partially supported by the Office of Naval Research and the NASA Center of Space Terahertz Technology. The authors would also like to thank Nihad Dib for theoretical model contributions.

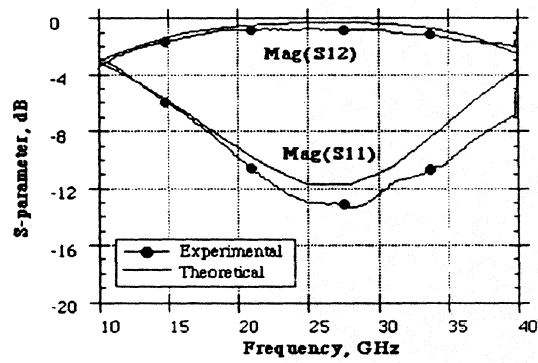
References

1. M. Yap, Y-C Tai, W.R. McGrath and C. Walker, "Silicon Micromachined Waveguides for Millimeter and Submillimeter Wavelengths," presented in the 3rd International Symposium on Space Terahertz Technology, Ann Arbor, MI, March 1992.
2. Linda P.B. Katehi, "Low-Loss Transmission Lines for Terahertz Frequency Applications," *IEEE Proceedings*, November 1992, pp.1771-1787.
3. N.I. Dib, P.B. Katehi, "Modeling of Shielded CPW Discontinuities Using the Space Domain Integral Equation Method (SDIE)," *Journal of Electromagnetic Waves and Applications (JEWA)*, Vol. 5, No 4 / 5, pp. 503-523.
4. N.I. Dib, L.P.B. Katehi, G.E. Ponchak and R.N. Simons, "Theoretical and Experimental Characterization of Coplanar Waveguide Discontinuities for Filter Applications," *IEEE Trans. on MTT*, Vol. 39, No. 5, May 1991.

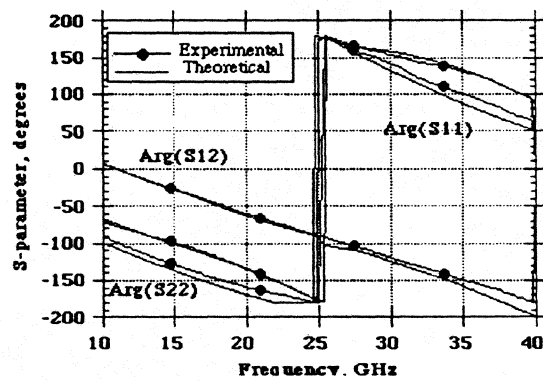
Figures



(a) Physical Geometry

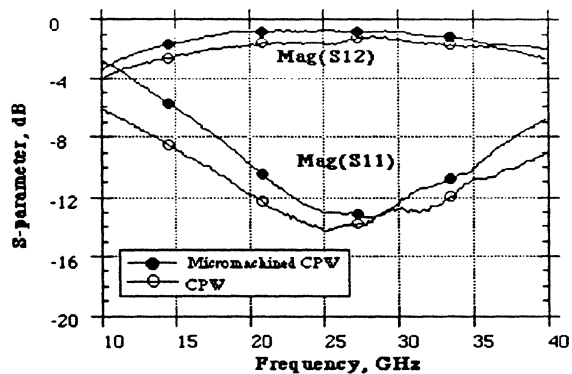


(a) Magnitude of Scattering Parameter

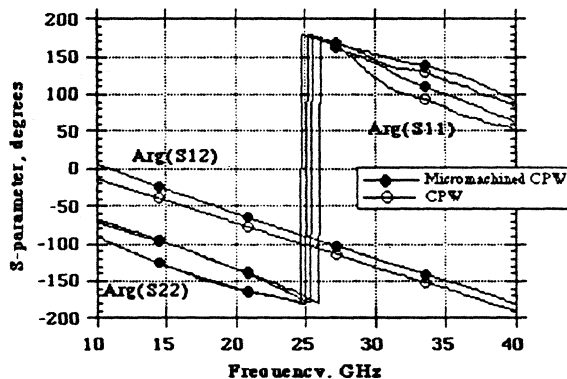


(b) Phase of Scattering Parameter

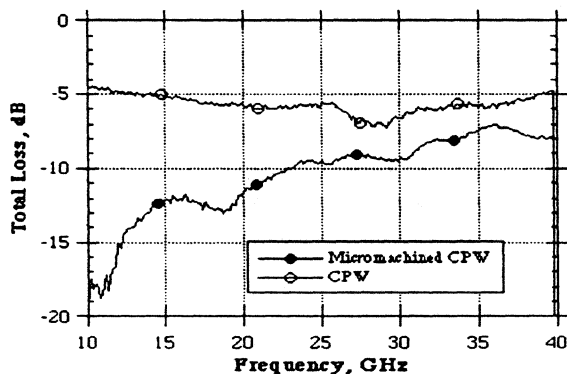
FIGURE A1. Micromachined CPW, Theoretical vs. Experimental: Open End Series Stub



(a) Magnitude of Scattering Parameters

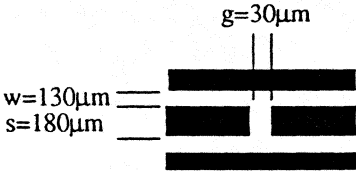


(b) Phase of Scattering Parameters

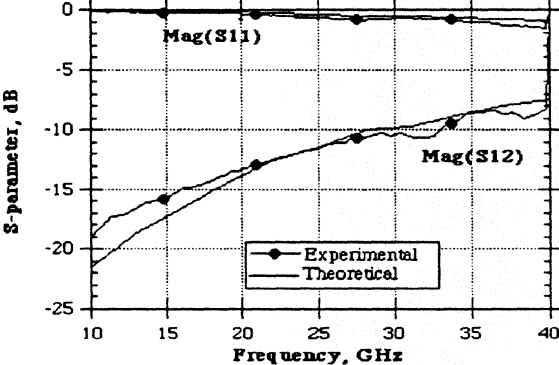


(c) Total loss

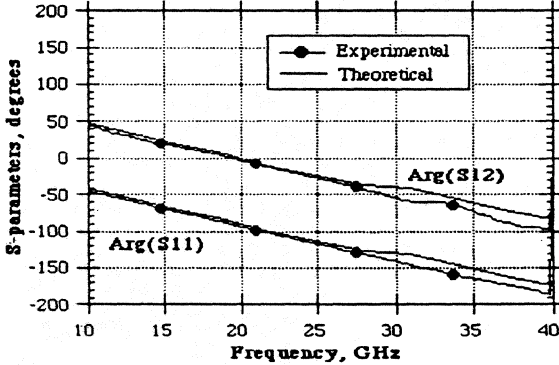
FIGURE A2. Micromachined CPW vs. CPW Line: Open End Series Stub



(a) Circuit geometry

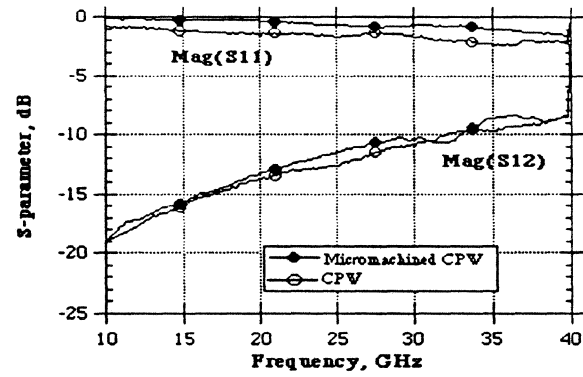


(b) Magnitude of scattering parameters

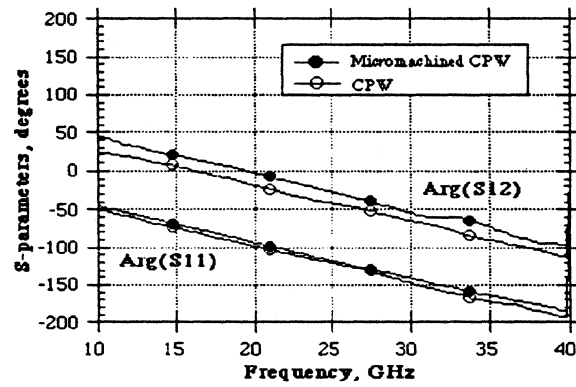


(c) Phase of scattering parameters

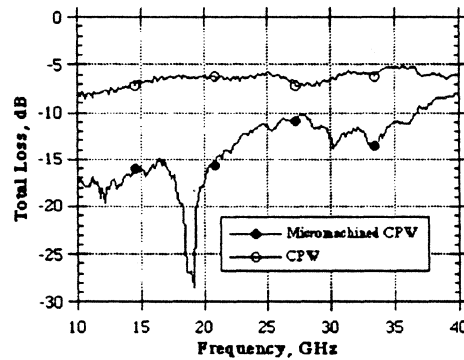
FIGURE B1. Micromachined CPW, Theoretical vs. Experimental: Open End Gap



(a) Magnitude of Scattering Parameters



(b) Phase of Scattering Parameters



(c) Total Loss

FIGURE B2. Micromachined CPW vs. CPW Line: Open End Gap